Observation of type-II recombination in single wurtzite/zinc-blende GaAs heterojunction nanowires

Neimantas Vainorius,[1] Daniel Jacobsson,[1] Sebastian Lehmann,[1] Anders Gustafsson,[1] Kimberly A. Dick,[1,2] Lars Samuelson,[1] and Mats-Erik Pistol[1,*]

[1]*Solid State Physics/The Nanometer Structure Consortium, Lund University, P.O. Box 118, SE-221 00 Lund, Sweden*

[2]*Center for Analysis and Synthesis, Lund University, P.O. Box 124, SE-221 00 Lund, Sweden*

(Received 6 December 2013; revised manuscript received 6 April 2014; published 28 April 2014)

We have investigated a large set of individual wurtzite/zinc-blende GaAs heterojunction nanowires using transmission electron microscopy (TEM), photoluminescence (PL), and cathodoluminescence (CL). In several cases we have combined PL and TEM on the same wire. We find a fairly deep emission that shows a strong blueshift with increasing excitation power density. By using a variety of experiments we show that this emission is due to recombination across a heterojunction with a type II band alignment. The data give a valence band offset of about 100 meV, in excellent agreement with theoretical predictions. Spatially resolved CL data on heterojunction nanowires and PL data on pure wurtzite nanowires show that the band gap of wurtzite GaAs is very close to the band gap of zinc-blende GaAs.

DOI: 10.1103/PhysRevB.89.165423 PACS number(s): 73.40.Kp, 78.55.Cr

I. INTRODUCTION

Semiconductor nanowires grown using III-V materials have a potential to become interesting building elements for future electronic and optoelectronic devices [1]. One of their most attractive properties is the possibility to combine highly lattice mismatched materials without the introduction of structural defects [2], allowing very flexible design rules for band structure engineering. In addition to this, nanowires can often be grown in either the wurtzite (wz) or the zinc-blende (zb) crystal phase, despite the fact that only the zinc-blende phase is found in bulk for non-nitride III-V materials [3] unless grown under nonequilibrium conditions and high pressure [4]. This opens up even more possibilities for band structure and heterojunction engineering. A challenge for band structure engineering is that the fundamental materials properties of the wurtzite crystal phase are not well known. As an example, the band gap of the wurtzite crystal phase of GaAs (wz-GaAs) is still under debate. The experimental determination of the wurtzite GaAs band gap ranges from 1.44 eV to 1.54 eV [5–9], whereas *ab initio* calculations result in band gaps between 1.38 eV and 1.81 eV [10–12]. Even less is known about the properties of heterojunctions between wurtzite and zinc-blende III-V materials, where the valence band offset is the fundamental parameter. In the GaAs case, it is believed that the heterojunction between wz-GaAs and zb-GaAs is type II, with the band edges of zb-GaAs being about 100 meV lower in energy than the band edges of wz-GaAs [9,12–14]. The potential discontinuity in type II heterojunctions causes a spatial separation of the charge carriers, where electrons are confined in one material and holes in the other. This gives rise to unusual photoluminescence (PL) behaviors, such as a strong energy dependence of emission peaks as a function of excitation power density [15,16] and long carrier lifetimes even if the constituent materials have a direct band gap [17]. This is advantageous for certain optoelectronic applications, especially photovoltaics [17]. In this paper we present photoluminescence (PL), cathodoluminescence (CL), and transmission electron microscopy (TEM) studies of pure wz-GaAs-zb-GaAs nanowires. The nanowires contain one wurtzite segment and one zinc-blende segment and have sharp interfaces between the two segments [18]. The nanowires are capped by $Al_xGa_{1-x}As$ ($x \approx 0.2$) in order to increase the luminescence yield. We often studied the same nanowire using both PL and TEM in order to correlate the structural and optical properties. As control samples we measured wz-GaAs nanowires capped with $Al_xGa_{1-x}As$ ($x \approx 0.2$). Another set of control samples consisted of a heterojunction of wz-GaAs and zb-GaAs which was not capped by AlGaAs. A PL peak below the band gap of both wz-GaAs and zb-GaAs which blueshifts with increasing excitation power density was consistently observed in the heterojunction wires, which is typical for recombination across a type II heterojunction [16]. This was confirmed by low temperature CL studies which show that the sub-band gap emission peak indeed originates from the interface between the wz-GaAs and the zb-GaAs segments. A valence band offset of about 90–100 meV was found, using the energy range over which this peak shifts. We also found that the band gap of wz-GaAs and zb-GaAs are very close to each other both in the CL experiments on the heterojunction samples and in the PL experiments on the control samples. We did not find any evidence of significant emission from stacking defects in wz-GaAs and neither did we find that stacking defects are detrimental to the optical quality of the crystals.

II. EXPERIMENTAL DETAILS

Growth of wz-GaAs-zb-GaAs nanowires is described in detail in Ref. [18], with the difference that we here added an $Al_xGa_{1-x}As$ ($x \approx 0.2$) shell, using tritertiarybutylaluminum (TTBAl) as Al precursor. At the end of the wz-GaAs growth, both TMGa and AsH_3 were turned off while adjusting reactor pressure and precursor flows for shell growth. The AlGaAs shell was grown at 550 °C for 20 min using $\chi_{TMGa} = 1.1 \times 10^{-5}$, $\chi_{TTBAl} = 3.9 \times 10^{-5}$, and $\chi_{AsH_3} = 1.5 \times 10^{-4}$. After shell growth, the samples were cooled in AsH_3/H_2 atmosphere.

To investigate optical properties of single nanowires we used microphotoluminescence where the nanowires were deposited onto marked gold substrates. We could thus reliably return to the same nanowire for repeated measurements on

*mats-erik.pistol@ftf.lth.se

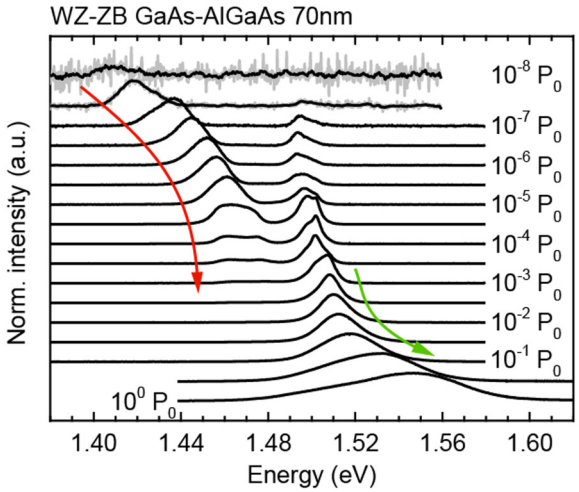

FIG. 1. (Color online) Photoluminescence spectra of one nanowire. The excitation power density is increasing from top to bottom. A peak which shifts in energy (red arrow), starting at about 1.41 eV at low excitation power density, can be seen as well as emission from the band edge (green arrow) at about 1.5 eV. At the highest excitation power densities the band edge emission blueshifts, due to the Burstein-Moss effect [19,20]. The spectra have been normalized to the strongest emission peak, giving the impression that the shifting peak becomes weak when it saturates. The black traces are smoothed, whereas the gray traces are raw data.

different days. All measurements were carried out at low temperature (7 K) in a continuous flow liquid helium cooled cold finger cryostat. We excited the samples using the 532 nm laser line of a frequency doubled yttrium-aluminium garnet (YAG) laser. The luminescence from the nanowires was collected by a microscope having a 20× objective, dispersed by grating monochromator and detected by a thermoelectrically cooled CCD camera. For the lowest excitation power densities we used about 1 h of integration time. We measured the excitation power dependence of 60 individual nanowires which were grown from aerosol produced gold particles with nominal diameters of 30 nm, 70 nm, and 80 nm. The nanowire diameter is somewhat larger than the gold particle diameter, but we will nevertheless refer to the nanowires by the diameter of the gold particle. About 30 control samples were measured.

The CL studies were carried out in a dedicated scanning electron microscope (SEM) equipped with a He-cold stage (7–9 K). The emission was dispersed by a monochromator and detected by a GaAs-photomultiplier tube to record spectra and monochromatic images. The nanowires were studied both as grown in sideview and transferred to Si substrates. To study spectral variations along individual nanowires, the electron beam was moved along the length and spectra were recorded at 50 nm intervals. We typically used an acceleration voltage of 5 kV and a probe current of 10 pA.

For high resolution TEM and x-ray energy dispersive spectroscopy (EDS) measurements, NWs were transferred to copper grids covered with a holey carbon layer by a direct mechanical transfer method, and investigated in a JEOL 3000 F TEM. For combined TEM and PL measurements, NWs were transferred to copper grids covered with continuous thin carbon film.

III. PHOTOLUMINESCENCE EXPERIMENTS

The PL experiments were carried out at different excitation power densities, varying over eight orders of magnitude. In Fig. 1 we show spectra from one nanowire having 70 nm diameter. Close to the zinc-blende band gap at 1.52 eV we observe a set of peaks which change in relative intensity with excitation power density. Some of these peaks are very likely due to point defects in the two segments and are slightly different for different wires. In addition, we observe a prominent peak that blueshifts with intensity, having an emission energy between 1.41 eV and 1.48 eV. This peak was present in all investigated heterojunction nanowires, although the intensity was different for different wires. The peak is split in many wires, which we will discuss below. A weak split can in fact be seen at intermediate excitation power density ($10^{-4}P_0$) in the spectra acquired for the nanowire presented in Fig. 1. We attribute the peak to recombination across a type-II heterojunction which are well known to have blueshifting peaks with increasing excitation power density [16]. The slope of the shift is not constant but decreases at intermediate power at the same time as the peak saturates in intensity. This decrease in slope with excitation power density is a general feature of the PL-probed nanowires and is also seen in Fig. 8 below. At the highest excitation power densities we find that the band edge emission blueshifts, due to state filling, i.e., a Burstein-Moss shift [19,20]. In Fig. 2 we show our interpretation of our results. At low excitation power

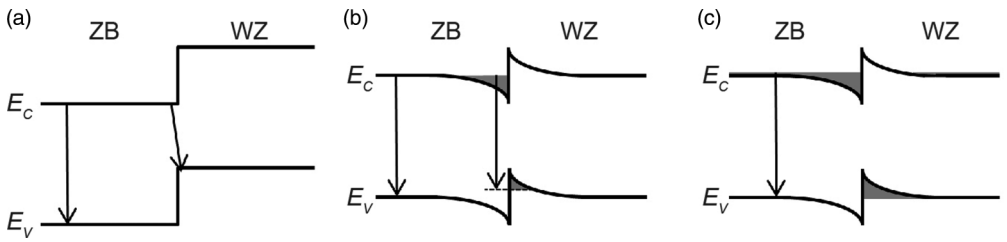

FIG. 2. Sketch of the band alignment at the zinc-blende/wurtzite GaAs heterointerface and type-II band-to-band transitions at low (a), intermediate (b), and high excitation power density (c). At low excitation power density we have emission from the heterojunction with an energy determined by the valence band offset between wz- and zb-GaAs. At intermediate excitation power density we get complete state filling of the electron potential well before the hole potential well is completely occupied. At the highest excitation power density both the electron and the hole potential wells are filled. At all excitation power densities we also have recombination of charge carriers across the band gaps. Note that the band gaps of wurtzite GaAs and zinc-blende GaAs are very close in energy in our samples.

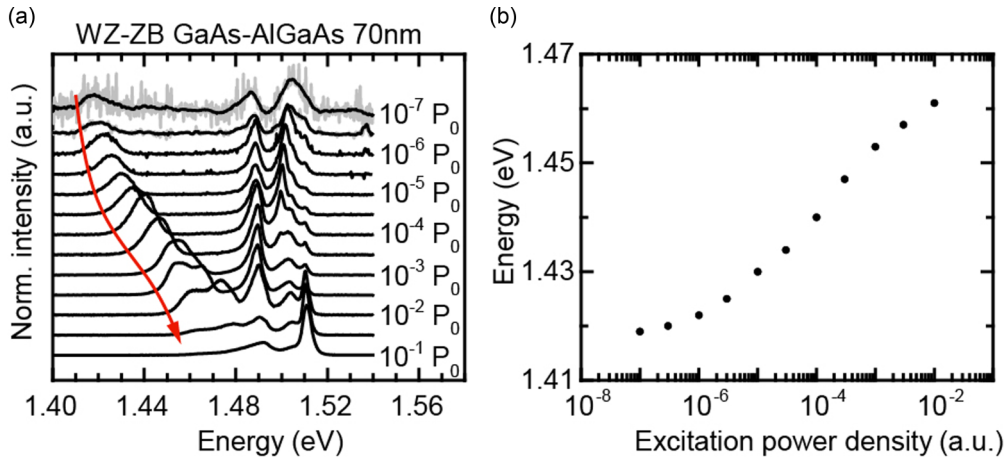

FIG. 3. (Color online) PL studies of 70 nm diameter NWs. PL spectra of a single nanowire investigated under a broad range of excitation power densities are shown in the left panel with the shifting peak indicated by a red arrow. The spectra were normalized to the highest intensity peak and plotted with an offset for clearer view. The emission energy of the shifting peak from the left panel is given as a function of the excitation power density in the right panel. The energy of the shifting peak was obtained by fitting the experimental peaks with a Gaussian line shape. The error bars are smaller than the plot points in the right panel. In the left panel the black traces are smoothed, whereas the gray traces are raw data.

density we have transitions across the type II heterojunction, Fig. 2(a). Simultaneously we have recombination across the band gaps of the two segments. With increasing excitation power density the bands start to align, similar to the case of an illuminated open circuit pn junction. This causes band bending at the interface, illustrated in Fig. 2(b). The band bending causes a triangular shaped potential well with confined states for carriers. Charge carriers will fill the triangular potential wells causing a Burstein-Moss shift of the emission peak. The highest energy electrons have the largest overlap with the holes, since the penetration of the wave function into the barrier increases with energy. The same is true for the holes and the dominant recombination is between the highest energy electrons and the highest energy holes (where the hole energy increases downward); see Fig. 2(b). This effect causes a PL peak where the emission energy shifts towards higher energy with increasing excitation power density. Since the density of states is much lower in the conduction band than in the valence band we will reach saturation of the state filling in the conduction band potential well first, illustrated in Fig. 2(b). At this point the energy shift of the shifting peak will become smaller since further state filling will only occur in the valence band potential well. Increasing the excitation power density further will cause state filling in the whole nanowire, which is also seen in the spectra in Fig. 1, corresponding to the highest excitation power densities.

Our explanation is unfortunately quite qualitative, but due to a lack of knowledge of the nanowire and materials properties such as recombination times, Fermi level pinning to the AlGaAs layer, density of states, etc., we cannot make a quantitative model. We mention that the Fermi level pinning on uncapped GaAs surfaces has been found to be different for

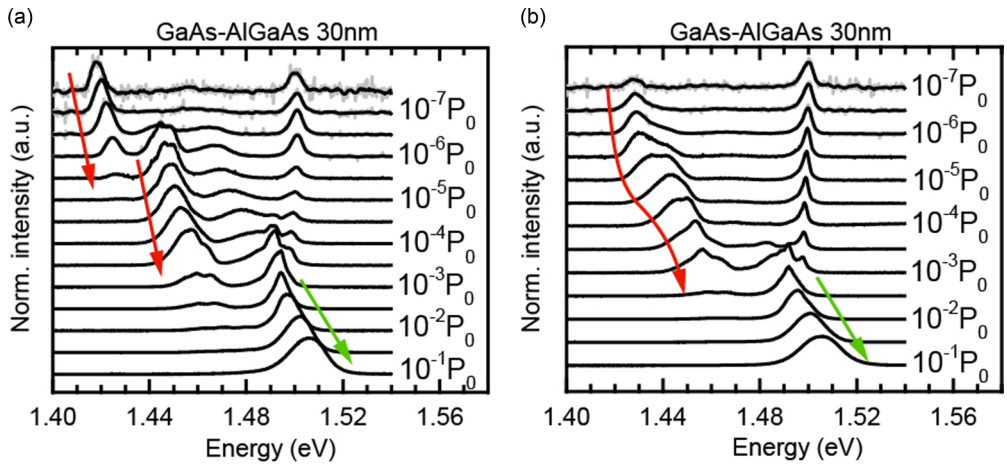

FIG. 4. (Color online) PL spectra of two 30 nm nanowires, where the excitation power density has been varied. Both wires show multiple shifting peaks, indicated by red arrows, which occurs at intermediate excitation power densities. The split between these peaks are different for different wires. At the highest excitation powers we observe a Burstein-Moss shift of the band edge emission, indicated by green arrows. The black traces are smoothed, whereas the gray traces are raw data.

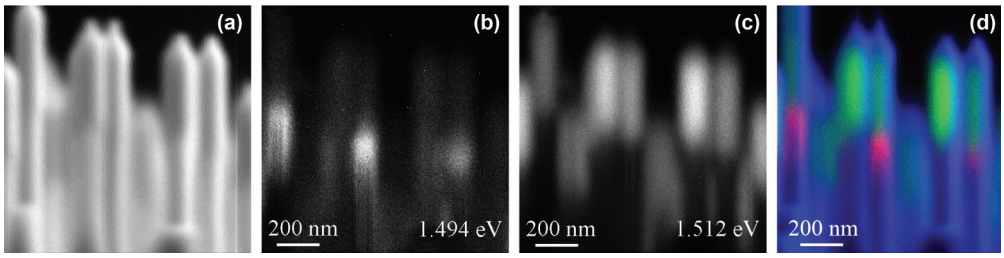

FIG. 5. (Color online) Scanning electron microscope (SEM) image (a); two CL images taken with detection energies of 1.494 eV (b) and 1.512 eV (c). The final panel (d) is a color-composite image, where blue is SEM, green is the 1.512 eV image, and red is the 1.494 eV image.

the two polytypes [21], although in samples very similar to ours this seems not to be the case [22]. At an excitation power density of $10^{-4}P_0$–$10^{-3}P_0$ we start to observe state filling in the whole wire and this should correspond to a carrier density of about 10^{18} cm^{-3}. An excitation power of $10^{-6}P_0$ should then correspond to a carrier density of at least 10^{16} cm^{-3}, which is enough to cause band bending given a background electron concentration of about 10^{16} cm^{-3} (Ref. [22]). This calculation is very rough and should only be taken as a sanity check. Our model gives a few predictions. At low energy there should be a limiting energy as can be seen in Fig. 2(a), corresponding to the band gap of zb-GaAs minus the valence band offset with respect to wz-GaAs. Figure 3 shows spectra from a nanowire where this limit was observed. At low energy we find that the limiting energy is about 1.42 eV in this wire. For other nanowires we find that we can sometimes reach a lower value of about 1.41 eV. Given a band gap of 1.52 eV for zb-GaAs and a low energy limit of 1.41–1.42 eV, we thus get a valence band offset of about 100 meV. This is close to the valence band offsets that have been discussed in the literature both from the experimental and the theoretical side [9,12–14].

We will now turn to a rather puzzling effect, the appearance of multiple shifting peaks, which is very often observed in our samples. In Fig. 4 we show spectra of two nanowires, having a 30 nm diameter, where multiple shifting peaks are more clearly seen than in the nanowires having a 70 nm diameter. From the figure it can be seen that there are several shifting peaks and that the transitions shifts from the deeper (lower energy) peaks to more shallow (higher energy) peaks with increasing excitation power density. This transition from deeper to shallower peaks with increasing excitation power density was observed in all nanowires where multiple peaks were observed. The presence of multiple peaks is not an exception; about 90% of the investigated nanowires have spectra with multiple peaks. The energy separation between the peaks is very dependent on wire, which can be seen in Fig. 4.

We propose three different explanations for the generation of multiple peaks in the PL spectra as follows:

(i) Multiple defects, where the shifting peak transition is not band to band but rather band to defect. For increasing excitation power density the deeper defects saturate and then the transition moves to the shallower defect.

(ii) Excited states of defects, where the shifting peak transition is again band to defect. For increasing excitation power density we saturate the ground state of the defect(s)

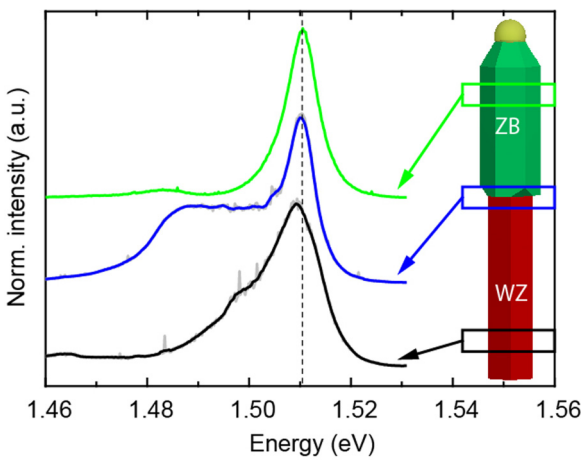

FIG. 6. (Color online) Spot mode spectra from three positions on the same single nanowire. The lower part is the wurtzite segment and the upper part is the zinc-blende segment. The colored traces are smoothed, whereas the gray traces are raw data.

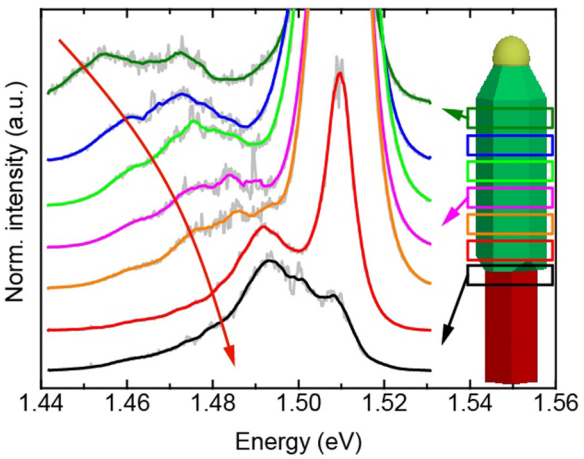

FIG. 7. (Color online) Cathodoluminescence spectra of one heterojunction nanowire. The excitation spot is at the heterojunction for the bottom spectra and was stepped towards the tip of the nanowire (in the zinc-blende segment) for successive spectra towards the top of the figure. The step size was 50 nm and the shifting peak is marked with a red arrow. The colored traces are smoothed, whereas the gray traces are raw data.

and the transition moves to the first excited state and so on.

(iii) Excited states in the triangular potential wells at the interface. Also here we saturate the ground state of the potential wells and the transition moves to the first excited state with increasing excitation power density.

All of these hypothesis imply further questions. If multiple defects are responsible, why does the emission from the deeper defect always become insignificant compared with the shallower defects at higher excitation power density? If defects are involved, the low energy limit should be very defect, and thus nanowire, dependent, but we essentially always observe a low energy limit of 1.41–1.42 eV, which, for instance, is the case for the nanowires shown in Figs. 1, 3, and 4. If the multiple peaks are due to excited states in the potential wells, we would expect a rather constant separation between the peaks from nanowire to nanowire, which is not observed. The separation between multiple peaks can easily differ a factor of 10 between different nanowires. Our favored explanation at this stage is that the multiple peaks are due to excited states in the potential wells. This means that the band bending is very different from nanowire to wire, causing the large scatter in peak separation between nanowires. Hopefully, we can return to this problem in a later investigation and propose more definite conclusions.

IV. CATHODOLUMINESCENCE EXPERIMENTS

In order to get further insight in the luminescence characteristics of GaAs wurtzite/zinc-blende heterostructured nanowires we carried out spatially resolved cathodoluminescence experiments. Nanowires with 70 nm diameter were investigated in side view geometry (90° tilt angle with respect to the substrate normal) while still standing on the substrate. The bottom of the nanowires is then the wurtzite segment and the top is the zinc-blende segment. Figure 5 shows a SEM image of nanowires in side view along with monochromatic CL images and a color composite. Detecting at 1.51 eV we find strong light emission located at the upper part of the nanowires (Fig. 5, depicted in green) corresponding to the expected band gap luminescence for the zinc-blende phase of GaAs. There is also emission from the wurtzite segment at this energy, but it is much weaker. Detecting at 1.49 eV we found an emission which is localized at the heterojunction, illustrated in Fig. 5. Figure 6 shows CL spectra from the two segments as well as

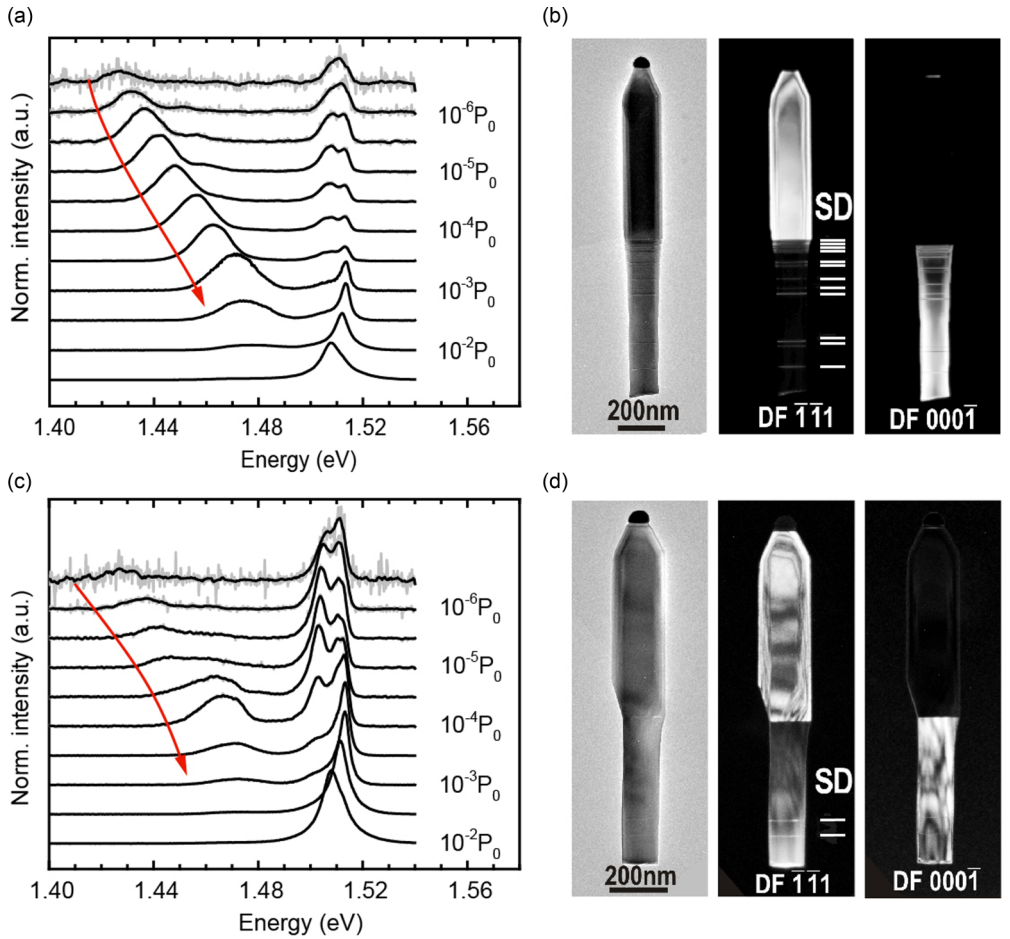

FIG. 8. (Color online) PL spectra of two 70 nm diameter nanowires and the corresponding bright field and dark field TEM images of the same nanowires. The dark field (DF) TEM images are taken at the indicated diffraction spots. Nanowire A, top panels (a), (b), has a set of stacking defects in the wurtzite segment (indicated by white lines), whereas the zinc-blende segment is without stacking defects. Nanowire B, bottom panels (c), (d), has only two stacking defects, both in the wurtzite segment. The shifting peak is indicated by red arrows. The black traces are smoothed, whereas the gray traces are raw data.

from the interface region. We see that the peak of the emission from the wurtzite segment is very close to the corresponding peak from the zinc-blende segment. We also note that the wurtzite emission is broader than the zinc-blende emission. The interface region shows a broad, quite strong emission, at 1.485 eV, which we attribute to the type II recombination.

In order to see if this emission is shifting, we would like to decrease the excitation power density. This we cannot do directly, since every absorbed electron will generate on the order of 1000 electron-hole pairs, defining the lowest possible excitation power density at the excitation spot. The beam current we use, 10 pA, corresponds to one electron every 10 ns. As an alternative method, we scanned the electron beam along the nanowire axis and took CL spectra, starting at the wurtzite/zinc-blende interface and moving upwards along the zinc-blende top segment. We then expect that the excitation power density at the heterojunction will decrease as the excitation spot moves further away. A 50 nm step size was used and the scan started at the heterojunction moving towards the tip of the nanowire, i.e., in the zinc-blende segment. Figure 7 shows the result. The emission localized at the heterojunction becomes weaker and redshifts, exactly as expected for our model and in perfect agreement with the PL results. When we moved the excitation beam in the wurtzite segment we did not see this effect cleanly, because the emission from the wurtzite segment is much broader than from the zinc-blende segment, masking the shifting peak.

V. COMBINED PL AND TEM MEASUREMENTS

In order to determine if extended defects such as stacking defects play any role in the luminescence spectra we combined PL and TEM measurements on the same wires. In Fig. 8 we show spectra along with TEM images of two wires, denoted A and B, respectively. No stacking defects are found in the zinc-blende segments and this is in fact the case for all 25 nanowires measured by TEM. The TEM images show that nanowire A has about 12 stacking defects in the wurtzite segment, whereas nanowire B has only two stacking defects in the wurtzite segment, and they are located far away from the interface. The PL intensity of the shifting peak in nanowire A is nevertheless somewhat stronger than in nanowire B despite having more stacking defects. It is tempting to assign the shifting peak to the stacking defects, but this is not supported by our control experiments. We have measured 15 nanowires in both PL and TEM but found no clear effect of the stacking defects; they do not seem to give any significant photoluminescence and they do not correlate with the occurrence of multiple peaks.

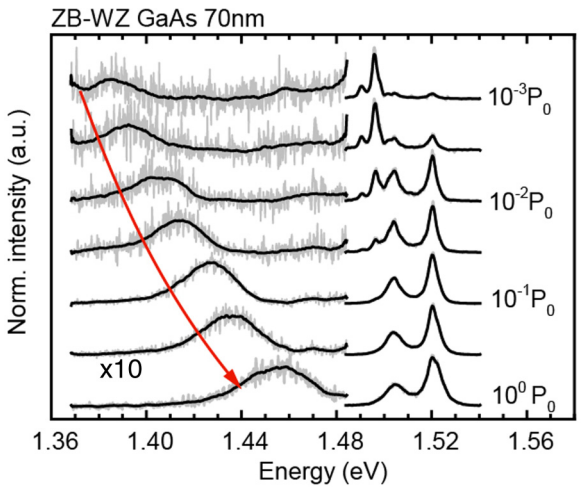

FIG. 9. (Color online) Photoluminescence spectra of a heterojunction nanowire grown without an AlGaAs shell for different excitation power densities. The shifting peak (red arrow) is quite weak in this sample compared with the band gap emission around 1.50–1.52 eV. The black traces are smoothed, whereas the gray traces are raw data.

VI. CONTROL EXPERIMENTS

Although the CL experiments give very strong support to our model of the shifting peak, we performed a set of control experiments. The first control experiment was to measure heterojunction nanowires which were not capped by AlGaAs. This was in order to exclude shifting peaks due to band

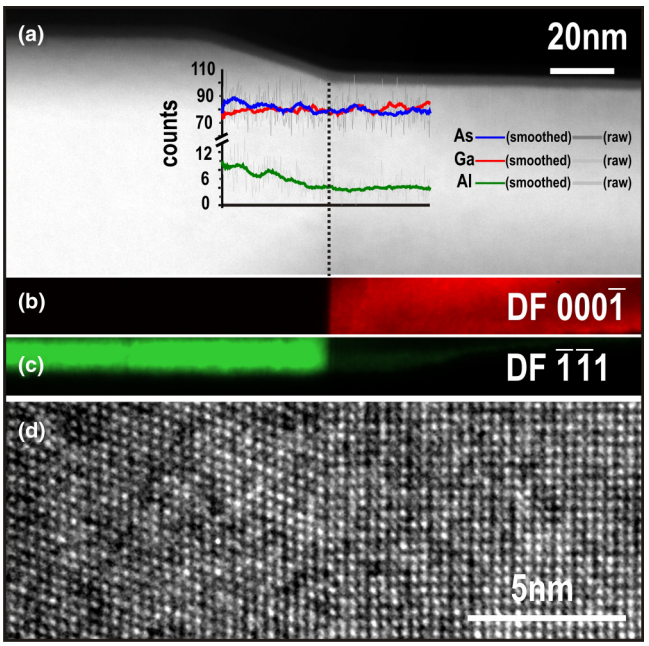

FIG. 10. (Color online) Scanning transmission electron microscopy (STEM) high angle annular dark field (HAADF) image of the transition region between wz-GaAs and the zb-AlGaAs (a). An axial segment of AlGaAs was formed during the AlGaAs shell growth. However, a STEM energy dispersive x-ray (EDX) line scan indicates that the position of the structural interface does not correspond to the compositional one as supported by the increase of the Al signal compared to the otherwise constant As signal. The structural interface was probed by dark field (DF) TEM images choosing the 000$\bar{1}$ double diffraction spot of the wz-GaAs and the $\bar{1}\bar{1}$1 spot for the zb-AlGaAs. The resulting DF images are given (false colored for better visualization) in (b) for wz-GaAs and in (c) for zb-GaAs with the same scale bar as (a). A high resolution TEM image (d) further indicates the sharp structural transition between the wurtzite and zinc-blende segments. (The growth direction of the wire was from right to left corresponding to the figure orientation.)

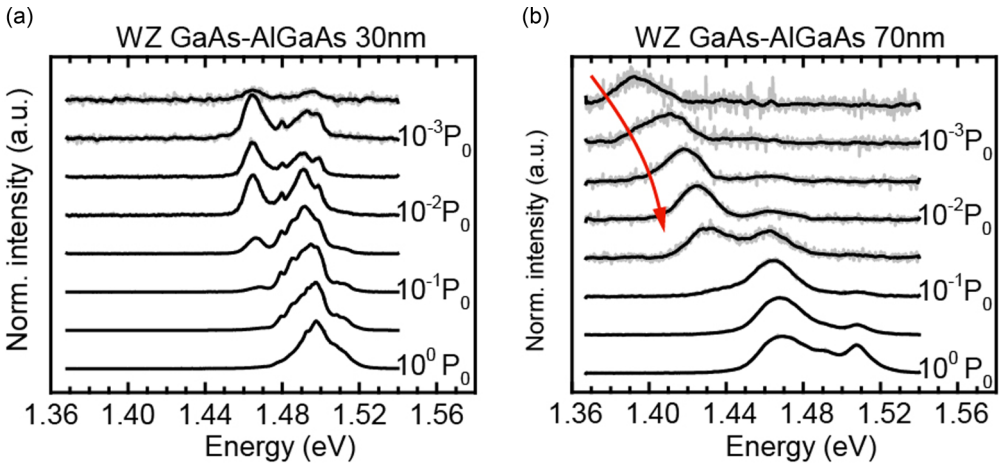

FIG. 11. (Color online) PL spectra of pure wurtzite GaAs nanowires. Left panel shows a PL spectra of a wurtzite GaAs nanowire with 30 nm diameter and the right panel the PL spectra of a GaAs nanowire with 70 nm diameter. The band gap emission is at about 1.51 eV in both nanowires, which is very close to the band gap emission of zinc-blende GaAs. For the thicker nanowire we observe a weak shifting peak, red arrow. This peak was never seen in the nanowires with 30 nm diameter. The black traces are smoothed, whereas the gray traces are raw data.

bending at the GaAs/AlGaAs interface which has recently been observed [23]. Figure 9 shows the result. Also in this nanowire we observe a shifting peak, although the relative intensity is quite weak. In fact the PL intensity in general is very weak in uncapped nanowires and this is why we most often measure capped wires.

The second set of control experiments was to measure PL on AlGaAs covered wz-GaAs nanowires. We carefully studied the interfacial region between the wz-GaAs and the axial segment of AlGaAs, which was formed during the shell formation process. We found a structural interface from wz-GaAs to a zb segment which is clearly to be seen from dark field (DF) (b),(c) and HRTEM (d) images in Fig. 10. Further, a XEDS line scan perpendicular to the structural interface indicates that although the structural transition is sharp, the compositional is not. An increase of the aluminum signal over about 30–40 nm with a decreasing gallium signal and a more or less constant arsenic signal can be found (a). (The aluminum signal which was detected at the wz-GaAs segment stems from the AlGaAs shell.) This overall means that a zb segment with a very low aluminum concentration forms the interface to the wz-GaAs. Figure 11 shows the photoluminescence spectra that we obtain. We measured ten nanowires with 30 nm diameter very carefully and in none of them could we find any shifting peaks. For the nanowires with 70 nm diameter we did find a (very weak) shifting peak in many of the wires. The intensity of the shifting peak in the reference samples is more than three orders of magnitude weaker than in the heterojunction samples. We attribute this weak peak to the short zinc-blende segment below the gold particle that we observe in TEM. A careful study of many nanowires by combined PL, CL, and TEM may give further clarification, but is not within the scope of this paper.

VII. CONCLUSION AND OUTLOOK

By carrying out a combination of photoluminescence, cathodoluminescence, and transmission electron microscopy we have determined the following:

(i) The heterojunction between wz-GaAs and zb-GaAs is type II, with a valence band offset of about 100 meV.

(ii) The band gap of wz-GaAs and zb-GaAs are essentially the same in our samples, to within a few meV as determined by photoluminescence. This is in agreement with resonant Raman scattering measurements by Ketterer *et al.*, who find that the excitonic band gap of the two polytypes is the same with an accuracy of better than 1 meV [7].

(iii) wz-GaAs emits much less than zb-GaAs, despite belonging to the same nanowire and having been grown under similar conditions [18].

(iv) A low density of stacking defects in wz-GaAs does not affect the photoluminescence to any significant degree. However, previous studies have shown that high densities of stacking defects give emission at an energy of about 1.49 eV in wz-GaAs [24].

Our results give some puzzling results that could be the subject of future research. We find for instance that the recombination across the heterojunction sometimes has multiple peaks which vary strongly between wires and the cause of this is unclear. The weak shifting emission in thicker wz-GaAs should be investigated more carefully, in order to make a definite statement of its origin. Why the band gap of wz-GaAs seems to vary between different research groups should also be studied more carefully.

ACKNOWLEDGMENTS

This work was performed within the nanometer structure consortium in Lund (nmC@LU) and supported by the Swedish Foundation for Strategic Research (SSF), nmC@LU, the Knut and Alice Wallenberg Foundation, and the Swedish Research Council (VR). S.L. gratefully acknowledges the support by a fellowship within the Postdoc-Programme of the German Academic Exchange Service (DAAD).

[1] X. Duan, Y. Huang, Y. Cui, J. Wang, and C. M. Lieber, Nature (London) **409**, 66 (2001).
[2] F. Glas, Phys. Rev. B **74**, 121302 (2006).
[3] P. Caroff, J. Bolinsson, and J. Johansson, Sel. Top. Quantum Electron. IEEE J. **18**, 18 (2010).
[4] M. I. McMahon and R. J. Nelmes, Phys. Rev. Lett. **95**, 215505 (2005).
[5] T. B. Hoang, A. F. Moses, H. L. Zhou, D. L. Dheeraj, B. O. Fimland, and H. Weman, Appl. Phys. Lett. **94**, 133105 (2009).
[6] D. C. Kim, D. L. Dheeraj, B. O. Fimland, and H. Weman, Appl. Phys. Lett. **102**, 142107 (2013).
[7] B. Ketterer, M. Heiss, E. Uccelli, J. Arbiol, and A. Fontcubertai Morral, ACS Nano **5**, 7585 (2011).
[8] L. Ahtapodov, J. Todorovic, P. Olk, T. Mjaland, P. Slattnes, D. L. Dheeraj, A. T. J. van Helvoort, B.-O. Fimland, and H. Weman, Nano Lett. **12**, 6090 (2012).
[9] M. Heiss, S. Conesa-Boj, J. Ren, H.-H. Tseng, A. Gali, A. Rudolph, E. Uccelli, F. Peiró, J. R. Morante, D. Schuh, E. Reiger, E. Kaxiras, J. Arbiol, and A. Fontcuberta i Morral, Phys. Rev. B **83**, 045303 (2011).
[10] Z. Zanolli, F. Fuchs, J. Furthmuller, U. von Barth, and F. Bechstedt, Phys. Rev. B **75**, 245121 (2007).
[11] C.-Y. Yeh, S.-H. Wei, and A. Zunger, Phys. Rev. B **50**, 2715 (1994).
[12] M. Murayama and T. Nakayama, Phys. Rev. B **49**, 4710 (1994).
[13] P. Kurananda, M. Montazeri, R. Gass, L. M. Smith, H. E. Jackson, J. Yarrison-Rice, S. Paiman *et al.*, Nano Lett. **9**, 648 (2009).
[14] A. Belabbes, C. Panse, J. Furthmuller, and F. Bechstedt, Phys. Rev. B **86**, 075208 (2012).
[15] J. Hu, X. G. Xu, J. A. H. Stotz, S. P. Watkins, A. E. Curzon, M. L. W. Thewalt, N. Matine, and C. R. Bolognesi, Appl. Phys. Lett. **73**, 2799 (1998).
[16] M. L. W. Thewalt, D. A. Harrison, C. F. Reinhart, J. A. Wolk, and H. Lafontaine, Phys. Rev. Lett. **79**, 269 (1997).
[17] S. S. Lo, T. Mirkovic, C.-H. Chuang, C. Burda, and G. D. Scholes, Adv. Mater. **23**, 180 (2011).
[18] S. Lehmann, D. Jacobsson, K. Deppert, and K. Dick, Nano Res. **5**, 470 (2012).
[19] E. Burstein, Phys. Rev. **93**, 632 (1954).
[20] T. S. Moss, Proc. Phys. Soc. B **67**, 775 (1954).
[21] P. Capiod, T. Xu, J. P. Nys, M. Berthe, G. Patriarche, L. Lymperakis, J. Neugebauer *et al.*, Appl. Phys. Lett. **103**, 122104 (2013).
[22] M. Hjort, S. Lehmann, J. Knutsson, R. Timm, D. Jacobsson, E. Lundgren, K. A. Dick, and A. Mikkelsen, Nano Lett. **13**, 4492 (2013).
[23] V. Dhaka, J. Oksanen, H. Jiang, T. Haggren, A. Nyknen, R. Sanatinia, J.-P. Kakko, T. Huhtio, M. Mattila, J. Ruokolainen, S. Anand, E. Kauppinen, and H. Lipsanen, Nano Lett. **13**, 3581 (2013).
[24] J. Bolinsson, M. Ek, J. Trägårdh, K. Mergenthaler, D. Jacobsson, M.-E. Pistol, L. Samuelson, and A. Gustafsson, Nano Research (2014), doi: 10.1007/s12274-014-0414-2.